

ORIGINAL ARTICLE

Brain Functional Organization Associated With Language Lateralization

Shuai Wang¹, Lise Van der Haegen², Lily Tao¹ and Qing Cai^{1,3,4}

¹Key Laboratory of Brain Functional Genomics (MOE & STGSM), Shanghai Changning-ECNU Mental Health Center, Institute of Cognitive Neuroscience, School of Psychology and Cognitive Science, East China Normal University, Shanghai 200062, China, ²Department of Experimental Psychology, Ghent University, Ghent B-9000, Belgium, ³Haskins Laboratories, 300 George Street, New Haven, USA and ⁴NYU-ECNU Institute of Brain and Cognitive Science at NYU Shanghai, Shanghai 200062, China

Address correspondence to Qing Cai, School of Psychology and Cognitive Science, East China Normal University, Shanghai 200062, China.
Email: miao.cai@gmail.com

Abstract

Although it is well-established that human language functions are mostly lateralized to the left hemisphere of the brain, little is known about the functional mechanisms underlying such hemispheric dominance. The present study investigated intrinsic organization of the whole brain at rest, by means of functional connectivity and graph theoretical analysis, with the aim to characterize brain functional organization underlying typical and atypical language dominance. We included healthy left-handers, both those with typical left-lateralized language and those with atypical right-lateralized language. Results show that 1) differences between typical and atypical language lateralization are associated with functional connectivity within the language system, particularly with weakened connectivity between left inferior frontal gyrus and several other language-related areas; and 2) for participants with atypical language dominance, the degree of lateralization is linked with multiple functional connectivities and graph theoretical metrics of whole brain organization, including local efficiency and small-worldness. This is the first study, to our knowledge, that linked the degree of language lateralization to global topology of brain networks. These results reveal that typical and atypical language dominance mainly differ in functional connectivity within the language system, and that atypical language dominance is associated with whole-brain organization.

Key words: functional connectivity, graph theory, language dominance, language lateralization, resting-state

Introduction

It is now well-established that human language functions are mostly lateralized to the left hemisphere of the brain. Left hemisphere language dominance has been observed for both the perception and production of speech, though the lateralization for speech perception seems to be less pronounced than that for production (Tzourio-Mazoyer et al. 2004; Van der Haegen and Cai 2018). Little is known, however, about the mechanisms underlying left language lateralization in the majority of healthy people. One speculation has been that the functional lateralization of language is triggered by sensory input. A recent study

investigated whether the absence of sensory input could change the hemispheric dominance of language (Van der Haegen et al. 2016). By assessing 7 congenital unilateral right-ear deaf participants, it was found that left hemisphere language dominance was preserved in this group, at a degree comparable to normal healthy populations. This suggests that the functional lateralization of language is not triggered by sensory input. Another line of research has investigated whether “function depends on structure.” However, no strong evidence has been found so far for a link between functional lateralization of language and anatomical asymmetries (Greve et al. 2013; Leroy et al. 2015; see Van

der Haegen and Cai 2018 for an overview of the main anatomical asymmetries in the human brain).

One reason for the difficulty in understanding the underlying mechanisms of functional lateralization is that the brain operates as a whole. Lateralization refers to the dominant hemisphere, which is by definition a dichotomous variable, that is, 1 of 2 possible values (3 when taking into account unclear dominance patterns). Practically, however, functions are underlay by complex networks engaging many brain regions, or, to put it in the extreme, brain regions composed of any number of neurons up to 86 billion in the whole brain. Therefore, analysis methods need to span the vast range in scale, and be able to bring a panoramic view.

Another aspect is that, while most psychological and neuroimaging studies exclusively examined right-handed healthy participants, the population with atypical functional lateralization involves mostly left-handed individuals, though the majority of left-handed individuals still show the typical left hemisphere dominance for language (Knecht et al. 2000). Left-handed populations with different language lateralization can offer unique perspectives for understanding the organization of language in the brain (Van der Haegen et al. 2012; Willems et al. 2014). Along this line, previous studies reported that visual word reading is consistently lateralized to the same hemisphere as speech production no matter which side it is (Cai et al. 2010; Van der Haegen et al. 2012), while complementary lateralization of speech production and visuospatial attention has also been found (Cai et al. 2013). These pieces of evidence indicate that language dominance and lateralization of other functions are not independent. In other words, when speech production is shifted to the right hemisphere, related functions would be expected to lateralize to the same hemisphere to achieve optimal information exchange, whereas unrelated functions may reside in the contralateral hemisphere (Cai et al. 2013). Given the tight relationships between these functional lateralization, language dominance should be related to the architecture of multiple functions and even whole-brain organization. However, whether and how the shift in language dominance is associated with changes in brain functional organization is yet unknown. It is important, therefore, to include left-handed groups in functional studies to understand how typical and atypical language dominance are associated with brain organization in healthy participants.

In the current study, we aimed to investigate the neural mechanisms of language dominance by looking at resting-state functional connectivity among left-handers with either typical or atypical language lateralization. Intrinsic brain organization at resting state is important for understanding functional organization, since it not only reflects cognitive architecture (Smith et al. 2009; Laird et al. 2011), but is also sensitive in capturing brain organization defined by anatomical connections (Honey et al. 2009; Hermundstad et al. 2013) or even by correlated gene expression (Richiardi et al. 2015). Specifically, a unique sample

of left-handers with either typical (left dominant; Ld) or atypical (right dominant; Rd) language lateralization was included in this study. The seed-based functional connectivity, functional connectivity density (FCD) mapping (Tomasi and Volkow 2010, 2012), and graph theory analysis (Bullmore and Sporns 2009; Rubinov and Sporns 2010) were performed on participants' resting-state fMRI data to characterize their brains' functional organization in terms of functional connectivity and network topology.

Methods

Participants

Participants were selected from a large group of 250 left-handers, who had previously been screened using behavioral visual hemi-field tasks to assess hemispheric language dominance (Van der Haegen et al. 2011). Those who showed clear left visual field advantage (indicating right hemispheric dominance), and those with right visual field advantage (i.e., left hemispheric dominance) were selected for recruitment in the current imaging study. Additionally, to better serve the purpose of the study, only those with clear functional language lateralization, as measured by the Lateralization Index (LI) under a speech production task (see below), were included ($LI > 0.6$). A total of 37 left-handers initially took part, 22 with left language dominance (Ld), and 15 with right language dominance (Rd). All participants had no history of psychiatric or neurological disorders, and gave written informed consent. Due to excessive head movement in the scanner, 4 Ld and 2 Rd were excluded. The final sample included 18 Ld (mean age 20.83, SD 2.94; 6 males) and 13 Rd (mean age 20.38, SD 2.81; 2 males). Handedness was assessed using an adapted version of the Edinburgh Handedness Inventory (Oldfield 1971), in which scores from -3 to -1 indicated a left manual preference. There were no significant differences between the 2 groups in age, gender, handedness scores, or degree of language lateralization (Fisher–Pitman permutation test; Table 1). The study was approved by the Ethics Committee of the Ghent University Hospital.

Word Generation Task and LI

A word generation task (WGT) was used to obtain the lateralization indices of speech production, to determine language dominance. During 10 blocks of 15 s each, participants mentally generated as many words as possible starting with a centrally presented target letter (experimental condition) or to silently repeat the nonexisting word “baba” (baseline condition). Experimental and control blocks were alternated by 20 blocks of 15 s rest. LI was calculated with the LI toolbox (Wilke and Lidzba 2007) using bilateral inferior frontal regions (pars opercularis and pars triangularis) as regions of interest (ROIs), and a Bootstrap method. The procedure of calculating LIs was the

Table 1 Characteristics of participant groups

	Ld (N = 18)	Rd (N = 13)	P-value
Age (years)	20.83 ± 2.94; 18–30	20.38 ± 2.81; 18 ~ 29	>0.71
Gender (M/F)	6/12	2/11	>0.41
Handedness	−2.41 ± 0.62; −3 ~ −0.9	−2.34 ± 0.78; −3 ~ −0.5	>0.79
Lateralization index	0.78 ± 0.09; 0.64 ~ 0.94	−0.81 ± 0.10; −0.93 ~ −0.62	(abs.) >0.48

Notes: Data are presented as mean ± SD; range.

same as for our previous study (Van der Haegen et al. 2012). Briefly, bootstrapped samples were taken in the left and right ROIs at a series of activation thresholds, only the central 50% of LI combinations of each individual were retained to avoid the influence of statistical outliers. A weighted mean LI were then calculated. Higher thresholds received higher weights in the resulting index to minimize the influence of arbitrarily chosen thresholds. The WGT was part of the acquisition of a large database including 7 other cognitive tasks in the scanner and a set of behavioral tasks, which are not further discussed in the present work. The mean LI for Ld was 0.78 (SD = 0.09), ranging from 0.64 to 0.94, with a higher value indicating more leftward inferior frontal gyrus (IFG) activation for speech production. The mean LI for Rd was -0.81 (SD = 0.10), ranging from -0.93 to -0.62, with a higher absolute value indicating more rightward IFG activation for speech production.

Image Acquisition and Preprocessing

Whole-brain images for the left-handers were acquired on a 3-T Siemens Trio MRI scanner (Siemens Medical Systems, Erlangen, Germany) with an 8-channel head coil, at the Ghent University Hospital. Anatomical images were obtained using a T1-weighted 3D MPRAGE sequence (TR = 1550 ms, TE = 2.39 ms, image matrix = 256×256 , FOV = 220 mm, flip angle = 9° , voxel size = $0.9 \times 0.9 \times 0.9$ mm³). Functional images were collected using a T2*-weighted gradient-echo EPI sequence covering the whole brain (TR = 2630 ms, TE = 35 ms, 40 axial slices, image matrix = 64×64 , FOV = 224 mm, flip angle = 80° , slice thickness = 3.0 cm, distance factor = 17%). For each participant, resting-state scanning lasted 7 min, with a total of 160 volumes scanned. During the resting-state run, participants were instructed to lie quietly with their eyes closed, and not to think of anything in particular. Preprocessing of resting-state fMRI data was performed using AFNI software (Cox 1996). The first 10 resting-state volumes were removed. Extreme time-series outliers were replaced through interpolation by using AFNI's 3dDespike. Slice-timing and head motion were corrected. Volumes were then coregistered to the anatomical image, normalized to MNI space, and resampled to 3 mm isotropic voxels. Nuisance regression was performed by using the basic ANATICOR method (Jo et al. 2010). The 6 head motion parameters, their derivatives and the first 3 principal components of CSF signals were regressed out. A band-pass filter (0.01–0.1 Hz) was applied. Global signal was not included in the nuisance regression given that this may introduce anticorrelation into the data (Murphy et al. 2009). Volumes with frame-wise displacement (FD) >0.3 mm or with >10% outliers of all voxels were censored along with the volume prior. Participants with >4% censored volumes or >0.1 mm averaged FD were excluded from further analysis.

Imaging Data Analysis

To fully describe functional organization of the brain, 3 types of functional connectivity measures were included, which are seed-based functional connectivity (RSFC; to examine functional organization at the region-to-region level), FCD (to examine functional organization at the region-to-brain level), and graph theoretical measures (to examine functional organization at the whole-brain level).

RSFC and FCD

A gray matter mask was extracted from the MNI-152 template (AFNI's MNI152_2009_template), and then intersected with its

flipped version to make a symmetrical mask. This symmetrical gray matter mask was spatially unbiased for both Ld and Rd groups, and was used as gray matter mask for next analysis. Two seed ROIs, namely bilateral inferior frontal regions (pars opercularis and pars triangularis), were defined through the procedure described previously (Van der Haegen et al. 2012), and constrained by the symmetrical gray matter mask (see Fig. S1). The mean time-series of each seed were calculated by averaging all voxels within the seed region, and then submitted into the next step for estimating seed-based voxel-wise resting state functional connectivity (RSFC) maps for each subject by using AFNI's 3dTcorr1D. These seed-based RSFC maps were converted to z-value maps through Fisher's *r*-to-*z* transformation for further statistical analysis. Unlike seed-based functional connectivity, the FCD mapping approach allows us to capture the functional role (hubness) of a given region within the entire voxel-wise functional network and not just pairwise relationships between the given regions and other voxels in the brain. Three measures of FCD were estimated to characterize the network profile for each gray matter voxel, which are global FCD (i.e., degree centrality; gFCD), local FCD (lFCD), and long-range FCD (lrFCD; Tomasi and Volkow 2010, 2012; Craddock et al. 2016). Local (short-range) FCD reflects the functional hubness of a voxel within its locally connected cluster, while long-range FCD is defined as lrFCD = gFCD - lFCD, which reflects the functional hubness of a voxel with other distal voxels. The lFCD and lrFCD can capture the detailed hubness of a region (locally or distally) beyond the global FCD.

Graph Theoretical Analysis

The graph theoretical analysis used a set of 402 symmetrical ROIs (Di402) covering gray matter of the whole brain, with a radius of 7 mm (Di et al. 2014). These ROIs (Di402) were constrained by the symmetrical gray matter mask—ROIs with less than 10 voxels within the gray matter mask were removed—resulting in 322 nodes. ROI-to-ROI correlation matrices were calculated by using AFNI's 3dNetCorr (Taylor and Saad 2013), these Fisher-*z*-transformed matrices were then thresholded into an undirected binary matrix with a wide range of densities from 6% to 54% at intervals of 1%. The upper bound (54%) approximated the minimum density (54.77%) among densities of all individual networks excluding negative connections. The lower bound (6%) is the sparsest density at which the relative size of largest connected component (scale to maximum) of each individual network was higher than 90%, with no significant between-group difference. Several key global graph metrics were calculated to characterize network topology in terms of functional integration (global efficiency), functional segregation (local efficiency and modularity), and the balance between functional integration and segregation (small-world parameters). The local efficiency, global efficiency, clustering coefficient, and characteristic path length were normalized to the averaged value of the same measure in 100 null networks. Small-worldness (σ) is estimated by the ratio of normalized clustering coefficient (γ) and normalized characteristic path length (λ). Degree distributions were fitted for describing the network hubness and overall organization. Degree distribution competing models included a power law, $P(k) \sim k^{-\alpha}$, an exponential law, $P(k) \sim e^{-\alpha k}$, and an exponentially truncated power law, $P(k) = k^{\alpha-1} e^{-k/\beta}$, goodness-of-fit was compared using Akaike's information criterion (AIC). The mean Euclidean distance (d) over all pairs of connected regions was also calculated to describe spatial patterns of connections. Graph theory analysis

was performed using the Brain Connectivity Toolbox (<https://www.nitrc.org/projects/bct/>) and the “brainwaver” package in R (<https://cran.r-project.org/web/packages/brainwaver/>).

Statistical Analyses

All individual seed-based RSFC z-value maps and FCD maps were first spatially smoothed with FWHM of 8 mm, and used as dependent variables in the subsequent linear regression model: $Y = \beta_0 + \beta_1 \times \text{group} + \beta_2 \times \text{age} + \beta_3 \times \text{gender} + \beta_4 \times \text{handedness} + \epsilon$. We used 3dttest++ to carry out the group-level analyses and group comparisons, and included age, sex, and handedness as covariates to be controlled. The newest ClustSim method was used with 3dttest++ for multicomparison correction. The residual maps derived from the model were used for calculating Spearman's ρ between LI and functional connectivity measure by using 3dTcorr1D. For graph measures, statistical analyses were performed on the values at the sparsest density (6%), and the area under the curve (AUC) across the whole range of densities. Between-group comparisons were carried out via Fisher–Pitman permutation test with Monte Carlo simulation of 100 000 times. For the Rd group, correlations between LI and functional connectivity measures were calculated using the absolute values of LIs to aid interpretation, since their original LIs are negative.

Results

Functional Connectivity

Left IFG and right IFG were used as seeds to perform seed-based RSFC analysis. The mean RSFC patterns of left IFG are shown in Figure 1A. For both groups, left IFG showed highest connectivity with its neighbor regions in left frontal cortex, and contralateral frontal regions. The left temporal region, left parietal region, and left ventral occipito-temporal region were also strongly connected with left IFG, demonstrating the intrinsic organization of the language system for both Ld and Rd groups (Fig. 1A). However, significant between-group differences were found in RSFC maps of left IFG seed (Fig. 1B, AlphaSim < 0.05 with $P < 0.01$ and $k > 117$ face-to-face voxels), which revealed that RSFC with bilateral angular gyrus (AG), bilateral precuneus, right middle temporal gyrus (MTG), and left inferior parietal lobule (IPL, part of the left AG cluster) were stronger in Ld group than in Rd group. For right IFG seed, the RSFC patterns were similar in Ld and Rd groups, and no significant between-group difference was found. Three FCD measures (gFCD, lFCD, and lrFCD) were estimated for each gray matter voxel, and there was no significant between-group difference. These results demonstrated that the shift of language dominance is mainly associated with the functional connectivity profile of left IFG, and mainly involved language-related regions such as bilateral AG, right MTG, and left IPL.

Relationship Between LI and Functional Connectivity Measures

To explore the within-group effects of language lateralization on functional connectivity, we carried out correlation analyses on seed-based RSFC maps and FCD maps. The results showed significant Spearman's correlations (ρ) between LI and several functional connectivity measures in Rd group, but not in Ld group (Fig. 2 and Table 2, $P < 0.01$ and $k > 80$ face-to-face voxels). In Rd group, the results revealed that functional connectivity between the right IFG seed and left insula lobe was

negatively related to LI (Spearman's $\rho = -0.83$ for the mean RSFC in left insula cluster), while functional connectivity between the right IFG seed and left MTG (Spearman's $\rho = 0.74$ for the mean RSFC in left MTG cluster) or left AG (Spearman's $\rho = 0.8$ for the mean RSFC in left AG cluster) were positively related to LI. The results also showed that gFCD of right fusiform gyrus was positively related to LI, and lFCD of left precuneus was negatively related to LI.

Network Topology and Its Relations With LI

In terms of network topology, each individual network showed a small-world organization ($\sigma > 1$) and an exponentially truncated power law of degree distribution (Fig. 3). The exponentially truncated power law has 2 fitting parameters—the power law exponent α and the exponential cutoff β . The 2 parameters α and β indicate the shape of degree distribution, for example, increased α and reduced β indicate that the probability of high degree node is reduced. While the group-comparison results showed no significant differences in any graph measures (see Table S1). However, a number of graph measures were significantly correlated with LI in Rd group (Fig. 4 and Table 3). Normalized local efficiency (E_{loc}) was positively correlated with LI (Spearman's $\rho = 0.69$ at sparsest density, and $\rho = 0.76$ for AUC), and normalized clustering coefficient (γ) was also positively correlated with LI (Spearman's $\rho = 0.73$ at sparsest density, and $\rho = 0.72$ for AUC). Due to the strong correlation between normalized clustering coefficient (γ) and LI and the absence of relation between normalized characteristic path length (λ) and LI, it is not surprising that network small-worldness (σ) was positively correlated with LI (Spearman's $\rho = 0.7$ at sparsest density, and $\rho = 0.73$ for AUC). In short, the results demonstrate that the greater the degree of atypical language lateralization (to the right hemisphere), the greater the extent of network segregation (local efficiency or clustering coefficient) and network small-worldness. Another graph measure of network segregation, modularity (Q), was also positively correlated with LI at sparsest density. Additionally, 2 fitting parameters of degree distribution, the power law exponent α and the exponential cutoff β , were significantly correlated with LI at sparsest density. The results showed that increased rightward laterality is related to higher α and lower β of degree distribution, indicating reduced probability of high degree hubs ($\rho = 0.6$ for α ; $\rho = -0.6$ for β).

Furthermore, to confirm the above results, 2 additional functionally defined ROI sets (Craddock400 and Craddock600) were extracted from the Craddock parcellations (Craddock et al. 2012), and used for the graph theoretical analysis with 337 nodes and 478 nodes respectively, after constraining by gray matter mask. Similar results were obtained by using the 2 additional schemes of network nodes, with no significant between-group difference and significant correlations between several graph theoretic measures and LIs in Rd group (see Table 3 for details) (Fig. 4).

Discussion

Using resting-state fMRI, we compared the functional brain organization of 2 groups of participants—left-handers with typical left language dominance and left-handers with atypical right language dominance. The main findings are summarized as follows. First, seed-based functional connectivity revealed that the shift in language dominance is associated with RSFC of

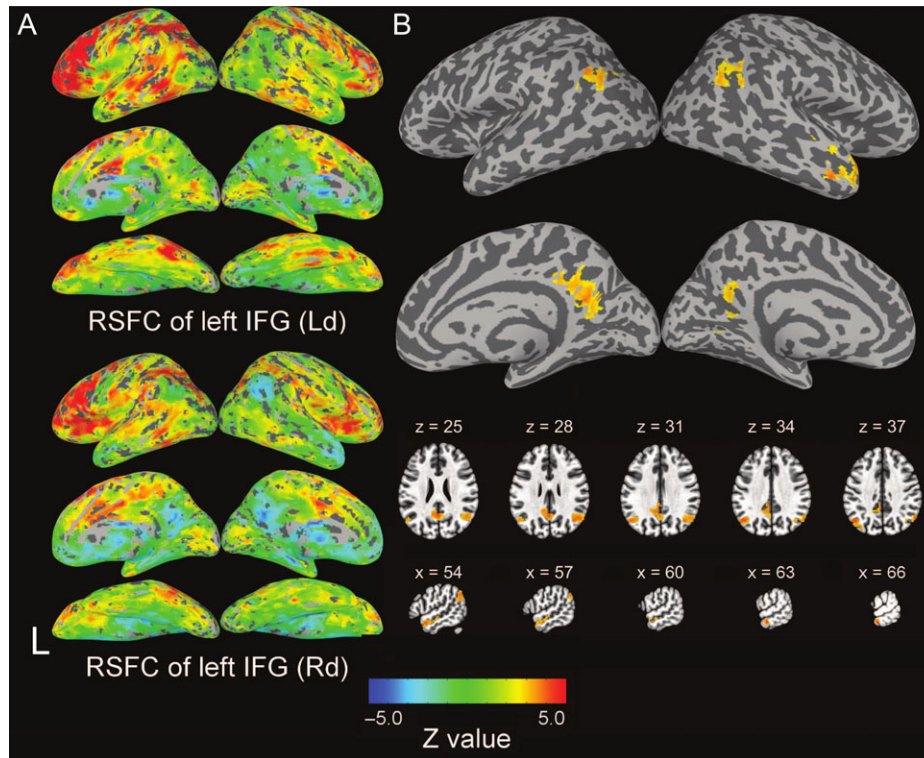


Figure 1. (A) The mean RSFC patterns of left IFG. The mean RSFC in Ld group was showed in the upper panel with lateral view, medial view, and ventral view (from top to bottom). The mean RSFC in Rd group was showed in the lower panel. (B) Between-group difference in RSFC of left IFG seed (AlphaSim <0.05 , with $P < 0.01$ and $k > 117$ face-to-face voxels). Compared with Rd group, the results show that Ld group has higher functional connectivity between left IFG and bilateral angular gyrus (AG), bilateral precuneus, right middle temporal gyrus (MTG), and left inferior parietal lobule (IPL).

left IFG with bilateral AG, with bilateral precuneus, with right MTG, or with left IPL, indicating that differences between typical and atypical language lateralization are reflected in the functional connectivity within the language system. Second, FCD and graph theoretical analysis showed no significant between-group difference, suggesting that the shift in language dominance is unrelated to global properties of brain organization. Third, the degree of language lateralization in the atypical group was found to be associated with RSFC of right IFG, gFCD, IFCD, and several graph measures of network topology, indicating that atypical language dominance has a link with whole-brain organization.

In regard to differences between typical and atypical language dominance, the results of reduced connectivity between left IFG and language-related regions in the Rd group suggest that atypical language dominance is associated with a weakened link between left IFG and leftward language system, including left AG and left inferior parietal regions connected by arcuate fasciculus (Catani et al. 2005), and right temporal cortex (right AG and right MTG). It is worth noting that there is no significant between-group difference in RSFC of right IFG, suggesting that right IFG in Rd group is not a functionally equivalent region as left IFG in Ld group, and that the language system in Rd group might involve language areas distributed in the 2 hemispheres but not directly shifted to the right hemisphere. This finding also suggests that there might be potential alterations in arcuate fasciculus among people with atypical language dominance. There is scope, therefore, for future studies to further investigate the structural connectivity of these language-related regions, particularly by examining white matter axon bundles or tracts, which have not been studied in

previous work in relation to language lateralization. High Angular Resolution Diffusion Imaging (HARDI), for example, could be employed to provide more robust delineation of white matter tracts. Through the combined analysis of functional and structural connectivity, we would be able to investigate the neural mechanisms underlying language dominance in greater depth.

Within the atypical Rd group, we found relationships between the degree of language lateralization (as indicated by LI) and several functional connectivity measures. Increased rightward laterality was associated with higher connectivity of right IFG to left MTG and left AG, indicating a strengthened link between right IFG and leftward language system. Given the between-group differences aforementioned, these results suggest an altered language system in Rd in terms of functional connectivity. Higher degree of rightward laterality was also associated with decreased connectivity between right IFG and left insula. Left insula has been reported to play a role in speech production of the leftward language system (Oh et al. 2014), and to be linked with Broca's area directly as an interface between Broca's area and cerebellum/basal ganglion (Eickhoff et al. 2009). When speech production shifted to the right hemisphere, right IFG could reduce functional connection with left insula while enhancing functional connection with right insula to maintain normal functions.

Additionally, gFCD and IFCD were associated with degree of lateralization in the Rd group. Specifically, higher gFCD in right fusiform gyrus was associated with increased rightward laterality, while higher IFCD in left precuneus was associated with reduced rightward LI. Because of the colateralization of speech production and word reading (Van der Haegen et al. 2012),

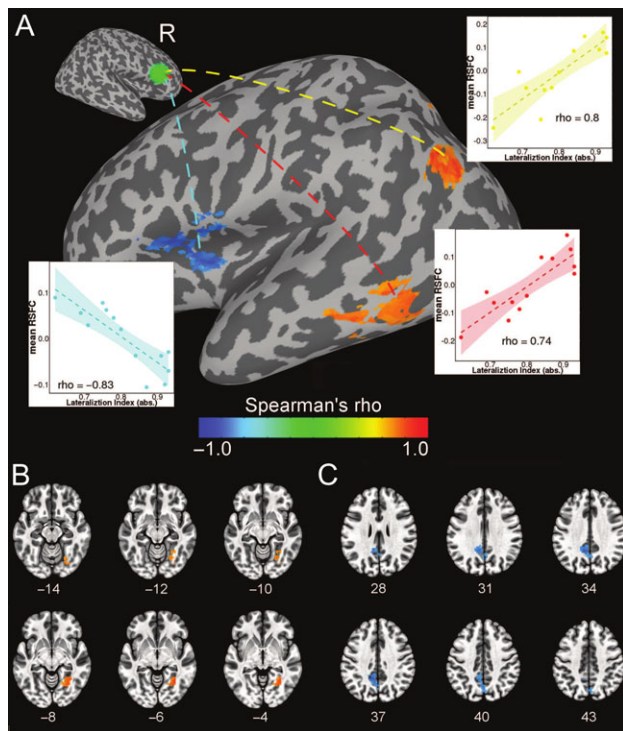


Figure 2. Relationships between language lateralization index and several functional connectivity and FCD measures (Spearman's ρ , $P < 0.01$ and $k > 80$ face-to-face voxels) in Rd group. (A) Functional connectivity between right IFG and left insula lobe was negatively correlated with LI, while functional connectivity between right IFG and left middle temporal gyrus (MTG) and left angular gyrus (AG) was positively correlated with LI. (B) global FCD in right fusiform gyrus was positively correlated with LI. (C) local FCD in left precuneus was negatively correlated with LI.

Table 2 Relationships between LI and functional connectivity measures in Rd group

	MNI coordinates (center of mass)			Volume (mm ³)
	X	Y	Z	
RSFC of right IFG seed				
Left insula lobe	-42.2	11.5	4.2	4347
Left middle temporal gyrus	-61.8	-41.5	-13.1	3348
Left angular gyrus	-45.6	-67.2	37.1	3159
Global FCD				
Right fusiform gyrus	26.6	-61.6	-10.4	2187
Local FCD				
Left precuneus	-5.2	-54.3	36.1	3672

increased rightward language dominance means more rightward word reading function, with higher involvement of right fusiform gyri. This atypical pattern might involve the right fusiform being functionally linked with numerous regions (such as face-processing regions and language system), resulting in a high amount of functional connections (gFCD). Precuneus has been reported to be involved in a number of cognitive functions such as visuospatial imagery, episodic memory retrieval and self-consciousness (Cavanna and Trimble 2006), and to be a functional hub in resting-state default-mode network (Raichle et al. 2001; Cavanna and Trimble 2006; Utevsy et al. 2014), and that task (compared with rest) might evoke increased

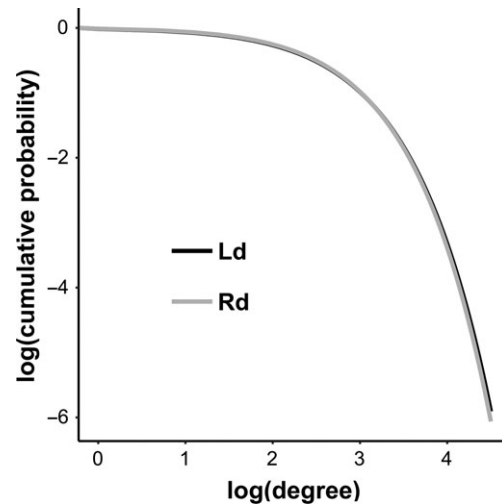


Figure 3. Cumulative degree distributions were best fitted by an exponentially truncated power law for both groups.

connectivity between the precuneus and the left frontoparietal network (Utevsy et al. 2014). The relationship between lFCD of left precuneus and LI in Rd group, along with the between-group difference in bilateral precuneus, gives us a hint that atypical language dominance might be associated with alterations of functional organization beyond the language system.

In terms of graph theoretical metrics, the observation of strong correlations between graph measures and LI in Rd is encouraging, since this is, to our knowledge, the first study showing brain network organization mechanisms underlying the degree, and not only the side, of language lateralization. For the Rd group, LI was significantly correlated with local efficiency (and clustering coefficient), that is, increased rightward laterality was associated with increased local efficiency of the whole-brain network. Local efficiency is related to fault tolerance at the local scale (Latora and Marchiori 2001), where higher local efficiency represents greater capacity of maintaining local communication in the topological network. Numerous studies have demonstrated that decreased local efficiency or clustering coefficient is associated with brain disorders, such as Alzheimer's disease (Supekar et al. 2008; Brier et al. 2014), Parkinson's disease (Luo et al. 2015), and schizophrenia (Liu et al. 2008; Alexander-Bloch et al. 2010; Lynall et al. 2010; Lo et al. 2015). Increased local efficiency (clustering coefficient) with unchanged global efficiency (characteristic path length) means increased small-worldness of brain networks, and this linked strong atypical language dominance to a more efficient and balanced network organization compared with weak atypical dominance.

The relationship between degree distribution fitting parameters (i.e., α and β) and LI also indicated that stronger atypical language dominance is associated with better brain network organization. The results of degree distribution demonstrated that participants with higher rightward laterality have reduced probability of high degree hubs. Brain network hubs have been associated with higher cerebral blood flow, metabolism, and energy demands (Vaishnavi et al. 2010; Liang et al. 2013; Tomasi et al. 2013), and increased sensitivity to brain disorders (Buckner et al. 2009; Crossley et al. 2014; Fornito et al. 2015). Hence, reduced probability of high degree hubs could mean reduced biological costs and risk. Putting these together with the absence of relationships between LI and graph measures in

Table 3 Relationships between LI and graph measures in Rd group

	Sparsest density			Area under curve		
	Di402 (6%)	Craddock400 (7%)	Craddock600 (6%)	Di402 (6–54%)	Craddock400 (7–57%)	Craddock600 (6–55%)
α	0.60 ⁺	0.43	0.56	0.18	0.13	0.12
β	-0.60 ⁺	-0.43	-0.56	-0.27	-0.23	-0.27
E_{loc} (normalized)	0.69 [*]	0.53	0.70 [*]	0.76 [*]	0.71 [*]	0.77 [*]
γ	0.73 [*]	0.60 ⁺	0.66 [*]	0.72 [*]	0.60 ⁺	0.59 ⁺
σ	0.70 [*]	0.61 ⁺	0.69 [*]	0.73 [*]	0.55	0.55
Q	0.69 [*]	0.48	0.79 [*]	-0.12	-0.26	-0.10
d	-0.55	-0.45	-0.45	-0.53	-0.56	-0.54

Notes: Data are presented as Spearman's ρ (FDR correction, * $p < 0.05$, + $P < 0.08$).

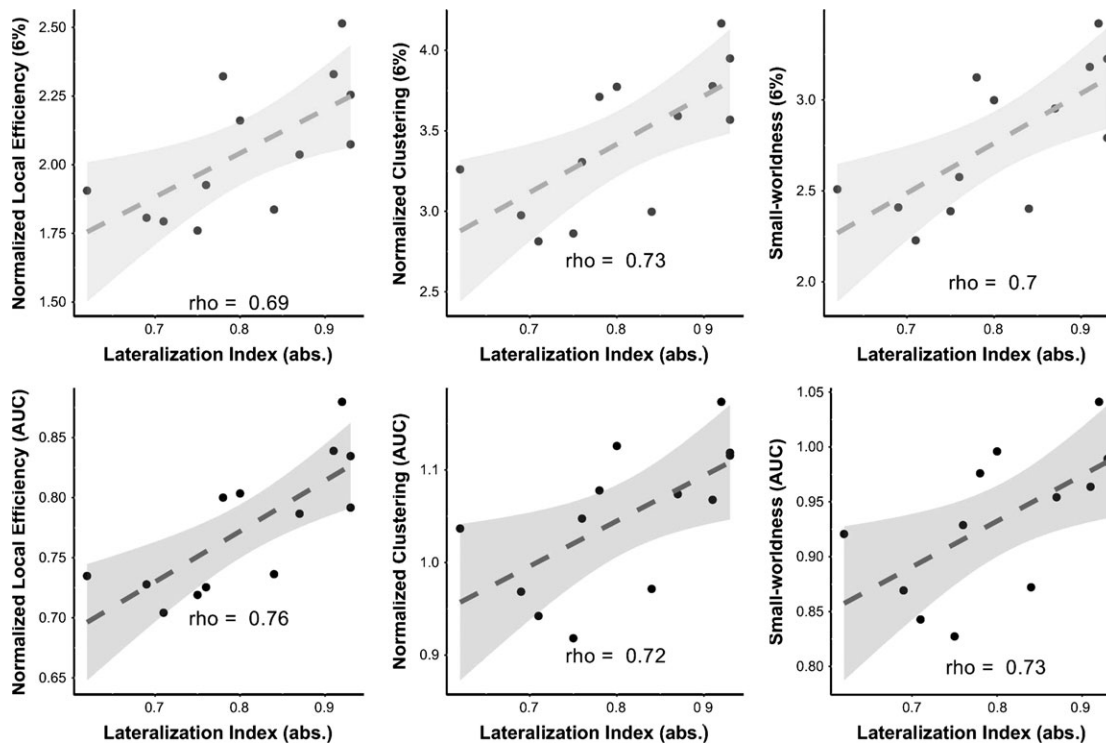


Figure 4. Relationships between language lateralization index and global graph measures (local efficiency, clustering coefficient, and small-worldness) at sparsest density (top row), and across the range of densities (area under the curve, AUC; bottom row).

the Ld group, we postulate that when the brain is atypically organized at the functional level, it might be protective to fully reverse the lateralization, rather than having weak lateralization, to minimize biological costs and avoid failure in functional organization. Additionally, our findings point to the importance of examining the degree of lateralization, in addition to the direction, in laterality studies. While most language functions show the same lateralization pattern in most humans, the degree of laterality can differ across functions and across individuals (Van der Haegen and Cai 2018). As such, the degree and direction of lateralization may not be “2 sides of the same coin,” but instead are 2 discrete variables. Differences in degree may, therefore, provide additional insights into the mechanisms underlying hemispheric dominance of functions.

A limitation in the current study is the left-handedness of our sample, and so does not allow examination of the effect of handedness and interaction between handedness and language dominance. Recent resting-state studies reported that intrahemispheric

connectivity asymmetries are mainly associated with hemispheric lateralization for language, but also shaped by handedness (Joliot et al. 2016; Tzourio-Mazoyer et al. 2016). However, this is a trade-off for us since right-handers with atypical language dominance are rare, and it would be clearer when we focus on language dominance rather than considering language dominance and handedness. Secondly, we did not perform voxel-wise graph theory analysis due to limited computing resource, instead we carried out FCD mapping and ROI-based graph theory analysis.

In sum, our results show that typical and atypical language dominance differ in functional connectivity between left IFG and mostly language-related regions, but not in global properties of whole-brain organization. Within the group with atypical language dominance, the degree of language lateralization was associated with local efficiency and small-worldness of brain networks, as well as several functional connectivity and FCD measures, indicating a link with whole-brain organization. Our findings point to the importance of examining the degree

of lateralization, in addition to the direction, in laterality studies, which would provide further insights into the mechanisms underlying hemispheric lateralization of functions. Further studies investigating structural connectivity will also be beneficial for understanding the mechanism underlying the language system and its lateralization.

Supplementary Material

Supplementary material is available at *Cerebral Cortex* online.

Funding

National Natural Science Foundation of China (NSFC 31771210 and 31400965 to Q.C.), Science and Technology Commission of Shanghai Municipality (17JC1404105 to Q.C. and 18YF1407600 to L.T.), Shanghai Municipal Commission of Health and Family Planning (ZK2015B01) and the Programs Foundation of Shanghai Municipal Commission of Health and Family Planning (201540114).

Notes

We particularly thank Marc Brysbaert for his generous support during the past few years and advice on various aspects of this project. We are also grateful to Yongdi Zhou for all his support and suggestions throughout the project, and Guy Vingerhoets for useful discussions. The authors declare that there are no competing financial interests in relation to the work presented here. *Conflict of Interest*: None declared.

References

- Alexander-Bloch AF, Gogtay N, Meunier D, Birn R, Clasen L, Lalonde F, Lenroot R, Giedd J, Bullmore ET. 2010. Disrupted modularity and local connectivity of brain functional networks in childhood-onset schizophrenia. *Front Syst Neurosci.* 4:147.
- Brier MR, Thomas JB, Fagan AM, Hassenstab J, Holtzman DM, Benzinger TL, Morris JC, Ances BM. 2014. Functional connectivity and graph theory in preclinical Alzheimer's disease. *Neurobiol Aging.* 35:757–768.
- Buckner RL, Sepulcre J, Talukdar T, Krienen FM, Liu H, Hedden T, Andrews-Hanna JR, Sperling RA, Johnson KA. 2009. Cortical hubs revealed by intrinsic functional connectivity: mapping, assessment of stability, and relation to Alzheimer's disease. *J Neurosci.* 29:1860–1873.
- Bullmore E, Sporns O. 2009. Complex brain networks: graph theoretical analysis of structural and functional systems. *Nat Rev Neurosci.* 10:186–198.
- Cai Q, Paulignan Y, Brysbaert M, Ibarrola D, Nazir TA. 2010. The left ventral occipito-temporal response to words depends on language lateralization but not on visual familiarity. *Cereb Cortex.* 20:1153–1163.
- Cai Q, Van der Haegen L, Brysbaert M. 2013. Complementary hemispheric specialization for language production and visuospatial attention. *Proc Natl Acad Sci USA.* 110:E322–E330.
- Catani M, Jones DK, Ffytche DH. 2005. Perisylvian language networks of the human brain. *Ann Neurol.* 57:8–16.
- Cavanna AE, Trimble MR. 2006. The precuneus: a review of its functional anatomy and behavioural correlates. *Brain.* 129: 564–583.
- Cox RW. 1996. AFNI: software for analysis and visualization of functional magnetic resonance neuroimages. *Comput Biomed Res.* 29:162–173.
- Craddock RC, Bellec P, Margules DS, Nichols BN, Pfanmüller JP, Badhwar A, Kennedy D, Poline JB, Toro R, Cipollini B, et al. 2016. Optimized implementations of voxel-wise degree centrality and local functional connectivity density mapping in AFNI. *Gigascience.* 5:1–26.
- Craddock RC, James GA, Holtzheimer PE, Hu XP, Mayberg HS. 2012. A whole brain fMRI atlas generated via spatially constrained spectral clustering. *Hum Brain Mapp.* 33:1914–1928.
- Crossley NA, Mechelli A, Scott J, Carletti F, Fox PT, Mcguire P, Bullmore ET. 2014. The hubs of the human connectome are generally implicated in the anatomy of brain disorders. *Brain.* 137:2382–2395.
- Di X, Kim EH, Chen P, Biswal BB. 2014. Lateralized resting-state functional connectivity in the task-positive and task-negative networks. *Brain Connect.* 4:641–648.
- Eickhoff SB, Heim S, Zilles K, Amunts K. 2009. A systems perspective on the effective connectivity of overt speech production. *Philos Trans A Math Phys Eng Sci.* 367:2399–2421.
- Fornito A, Zalesky A, Breakspear M. 2015. The connectomics of brain disorders. *Nat Rev Neurosci.* 16:159–172.
- Greve DN, Van der Haegen L, Cai Q, Stufflebeam S, Sabuncu MR, Fischl B, Brysbaert M. 2013. A surface-based analysis of language lateralization and cortical asymmetry. *J Cogn Neurosci.* 25:1477–1492.
- Hermundstad AM, Bassett DS, Brown KS, Aminoff EM, Clewett D, Freeman S, Frithsen A, Johnson A, Tipper CM, Miller MB, et al. 2013. Structural foundations of resting-state and task-based functional connectivity in the human brain. *Proc Natl Acad Sci USA.* 110:6169–6174.
- Honey CJ, Honey CJ, Sporns O, Sporns O, Cammoun L, Cammoun L, Gigandet X, Gigandet X, Thiran JP, Thiran JP, et al. 2009. Predicting human resting-state functional connectivity from structural connectivity. *Proc Natl Acad Sci USA.* 106:2035–2040.
- Jo HJ, Saad ZS, Simmons WK, Milbury LA, Cox RW. 2010. Mapping sources of correlation in resting state FMRI, with artifact detection and removal. *Neuroimage.* 52:571–582.
- Joliot M, Tzourio-Mazoyer N, Mazoyer B. 2016. Intra-hemispheric intrinsic connectivity asymmetry and its relationships with handedness and language Lateralization. *Neuropsychologia.* 93:437–447.
- Knecht S, Drager B, Deppe M, Bobe L, Lohmann H, Floel A, Ringelstein EB, Henningsen H. 2000. Handedness and hemispheric language dominance in healthy humans. *Brain.* 123 (Pt 12):2512–2518.
- Laird AR, Fox PM, Eickhoff SB, Turner JA, Ray KL, McKay DR, Glahn DC, Beckmann CF, Smith SM, Fox PT. 2011. Behavioral interpretations of intrinsic connectivity networks. *J Cogn Neurosci.* 23:4022–4037.
- Latora V, Marchiori M. 2001. Efficient behavior of small-world networks. *Phys Rev Lett.* 87:198701.
- Leroy F, Cai Q, Bogart SL, Dubois J, Coulon O, Monzalvo K, Fischer C, Glasel H, Van der Haegen L, Bénézit A, et al. 2015. New human-specific brain landmark: the depth asymmetry of superior temporal sulcus. *Proc Natl Acad Sci USA.* 112: 1208–1213.
- Liang X, Zou Q, He Y, Yang Y. 2013. Coupling of functional connectivity and regional cerebral blood flow reveals a physiological basis for network hubs of the human brain. *Proc Natl Acad Sci USA.* 110:1929–1934.
- Liu Y, Liang M, Zhou Y, He Y, Hao Y, Song M, Yu C, Liu H, Liu Z, Jiang T. 2008. Disrupted small-world networks in schizophrenia. *Brain.* 131:945–961.

- Lo C-YZ, Su T-W, Huang C-C, Hung C-C, Chen W-L, Lan T-H, Lin C-P, Bullmore ET. 2015. Randomization and resilience of brain functional networks as systems-level endophenotypes of schizophrenia. *Proc Natl Acad Sci USA*. 112:9123–9128.
- Luo CY, Guo XY, Song W, Chen Q, Cao B, Yang J, Gong QY, Shang H-F. 2015. Functional connectome assessed using graph theory in drug-naive Parkinson's disease. *J Neurol*. 262:1557–1567.
- Lynall M-E, Bassett DS, Kerwin R, McKenna PJ, Kitzbichler M, Muller U, Bullmore E. 2010. Functional connectivity and brain networks in schizophrenia. *J Neurosci*. 30:9477–9487.
- Murphy K, Birn RM, Handwerker DA, Jones TB, Bandettini PA. 2009. The impact of global signal regression on resting state correlations: are anti-correlated networks introduced? *Neuroimage*. 44:893–905.
- Oh A, Duerden EG, Pang EW. 2014. The role of the insula in speech and language processing. *Brain Lang*. 135:96–103.
- Oldfield RC. 1971. The assessment and analysis of handedness: the Edinburgh inventory. *Neuropsychologia*. 9:97–113.
- Raichle ME, MacLeod AM, Snyder AZ, Powers WJ, Gusnard DA, Shulman GL. 2001. A default mode of brain function. *Proc Natl Acad Sci USA*. 98:676–682.
- Richiardi J, Altmann A, Milazzo AC, Chang C, Chakravarty MM, Banaschewski T, Barker GJ, Bokde AL, Bromberg U, Buchel C, et al. 2015. Correlated gene expression supports synchronous activity in brain networks. *Science*. 348:1241–1244.
- Rubinov M, Sporns O. 2010. Complex network measures of brain connectivity: uses and interpretations. *Neuroimage*. 52:1059–1069.
- Smith SM, Fox PTMTM, Miller KL, Glahn DC, Fox PTMTM, Mackay CE, Filippini N, Watkins KE, Toro R, Laird AR, et al. 2009. Correspondence of the brain's functional architecture during activation and rest. *Proc Natl Acad Sci USA*. 106:13040–13045.
- Supekar K, Menon V, Rubin D, Musen M, Greicius MD. 2008. Network analysis of intrinsic functional brain connectivity in Alzheimer's disease. *PLoS Comput Biol*. 4:e1000100.
- Taylor PA, Saad ZS. 2013. FATCAT: (an efficient) Functional and Tractographic Connectivity Analysis Toolbox. *Brain Connect*. 3:523–535.
- Tomasi D, Volkow ND. 2010. Functional connectivity density mapping. *Proc Natl Acad Sci USA*. 107:9885–9890.
- Tomasi D, Volkow ND. 2012. Resting functional connectivity of language networks: characterization and reproducibility. *Mol Psychiatry*. 17:841–854.
- Tomasi D, Wang G, Volkow N. 2013. Energetic cost of brain functional connectivity. *Proc Natl Acad Sci USA*. 110:13642–13647.
- Tzourio-Mazoyer N, Joliot M, Marie D, Mazoyer B. 2016. Variation in homotopic areas' activity and inter-hemispheric intrinsic connectivity with type of language lateralization: an fMRI study of covert sentence generation in 297 healthy volunteers. *Brain Struct Funct*. 221:2735–2753.
- Tzourio-Mazoyer N, Josse G, Crivello F, Mazoyer B. 2004. Interindividual variability in the hemispheric organization for speech. *Neuroimage*. 21:422–435.
- Utevsky AV, Smith DV, Huettel SA. 2014. Precuneus is a functional core of the default-mode network. *J Neurosci*. 34:932–940.
- Vaishnavi SN, Vlassenko AG, Rundle MM, Snyder AZ, Mintun MA, Raichle ME. 2010. Regional aerobic glycolysis in the human brain. *Proc Natl Acad Sci USA*. 107:17757–17762.
- Van der Haegen L, Acke F, Vingerhoets G, Dhooge I, De Leenheer E, Cai Q, Brysbaert M. 2016. Laterality and unilateral deafness: patients with congenital right ear deafness do not develop atypical language dominance. *Neuropsychologia*. 93:482–492.
- Van der Haegen L, Cai Q. in press. Lateralization of language. In: Zubicaray IG, Schiller N, editors. *Oxford handbook of neurolinguistics*. UK: Oxford University Press. p. 877–906.
- Van der Haegen L, Cai Q, Brysbaert M. 2012. Colateralization of Broca's area and the visual word form area in left-handers: fMRI evidence. *Brain Lang*. 122:171–178.
- Van der Haegen L, Cai Q, Seurinck R, Brysbaert M. 2011. Further fMRI validation of the visual half field technique as an indicator of language laterality: a large-group analysis. *Neuropsychologia*. 49:2879–2888.
- Wilke M, Lidzba K. 2007. LI-tool: a new toolbox to assess lateralization in functional MR-data. *J Neurosci Method*. 163:128–136.
- Willems RM, Van der Haegen L, Fisher SE, Francks C. 2014. On the other hand: including left-handers in cognitive neuroscience and neurogenetics. *Nat Rev Neurosci*. 15:193–201.